Turkish Journal of Electrical Engineering & Computer Sciences

http://journals.tubitak.gov.tr/elektrik/

Research Article

Turk J Elec Eng & Comp Sci
(2020) 28: 1121 – 1134

doi:10.3906/elk-1907-119

Design and characterization of a compact single-layer multibeam array antenna using an 8×8 Butler matrix for 5G base station applications

Intan Izafina IDRUS[1], Tarik ABDUL LATEF[1,*], Narendra Kumar ARIDAS[1], Mohamad Sofian ABU TALIP[1], Yoshihide YAMADA[2], Tengku Faiz TENGKU MOHMED NOOR IZAM[1], Tharek ABD RAHMAN[3]

[1]Department of Electrical Engineering, Faculty of Engineering, University of Malaya, Kuala Lumpur, Malaysia
[2]Department of Electronic Systems Engineering, Malaysia-Japan International Institute of Technology, University Teknologi Malaysia, Kuala Lumpur, Malaysia
[3]Wireless Communication Centre, Universiti Teknologi Malaysia, Johor Bharu, Johor, Malaysia

Received: 16.07.2019 • **Accepted/Published Online:** 16.10.2019 • **Final Version:** 28.03.2020

Abstract: A multibeam array antenna employing a Butler matrix is a promising solution for fifth generation (5G) base stations. Due to inaccurate phase differences between output ports in the Butler matrix, the radiation characteristics could show incorrect main beam directions. In addition, the literature has also reported the issue of high amplitude imbalance in the Butler matrix. This paper presents a single-layer multibeam array antenna fed by an 8×8 Butler matrix operating at 28 GHz for 5G base station applications—a more cost-effective solution for large-scale production. The Butler matrix consists of twelve quadrature hybrids, sixteen crossovers, and eight phase shifters. This circuit was integrated with eight antenna elements at the output ports of the Butler matrix. The proposed multibeam array antenna was fabricated using a low dielectric constant and a low loss tangent substrate. The dimensions of the multibeam array antenna were $88 \times 106 \times 0.254$ mm^3. The Butler matrix achieved low insertion losses and low phase error with average values of 2.5 dB and less than $\pm 10^\circ$ at 28 GHz, respectively. The measured return losses were less than -10 dB at 28 GHz. The measured radiation patterns were obtained and eight main beams were pointed at $\pm 6^\circ$, $\pm 18^\circ$, $\pm 30^\circ$, and $\pm 44^\circ$ with measured gains between 9 dBi and 14 dBi.

Key words: Base station, Butler matrix, fifth generation, 5G, multibeam array antenna, single-layer

1. Introduction

Research on fifth-generation (5G) mobile communication systems has attracted much interest from researchers and design engineers that wish to cater to the increasing demand for higher data rates and data traffic [1–3]. These efforts have been accelerated to meet the standardization of the International Telecommunications Union Radiocommunication by 2020 [4]. The main features of 5G mobile communication systems are the utilization of millimeter waves, the deployment of small cells with radius cells of 200 m, and the use of a multibeam base station antenna for multiple-input multiple-output (MIMO) schemes [5–7].

Multibeam array antennas play an important role in enhancing system capacity. This antenna also improves network coverage and reduces co-channel interference [5, 8]. Figure 1 illustrates a multibeam base station with each radiation beam assigned to one mobile user. To achieve the multibeam characteristic, beamforming circuits such as the Butler matrix, the Rotman lens, and the Blass matrix can be fed to the array

*Correspondence: tariqlatef@um.edu.my

antenna [9–11]. The Butler matrix has received much attention due to its low profile, low power dissipation, design simplicity, and cost-effectiveness for large-scale production [12–16]. The Rotman lens suffers high ohmic loss, high power loss within the lens, and high phase error across the aperture, although it is low-profile and cost-effective, and it has wider bandwidth [17, 18]. The Blass matrix has low efficiency due to high losses associated with the structure [19]. In addition, the Butler matrix has the ability to produce orthogonal beams, which improve the beam scanning coverage [20]. Therefore, the Butler matrix is chosen as beamforming circuit in this work. The configuration of a base station antenna is presented in Figure 2. The antenna structure is compact and suitable for use in a space-constrained base station. The main drawback in designing a Butler matrix in millimeter waves using microstrip technology is inaccurate beam directions, especially for higher-order Butler matrices, as the length of a microstrip line corresponds to a phase change. To overcome this issue, a Butler matrix must have high accuracy dimensions to ensure that the radiation beams point in the desired directions.

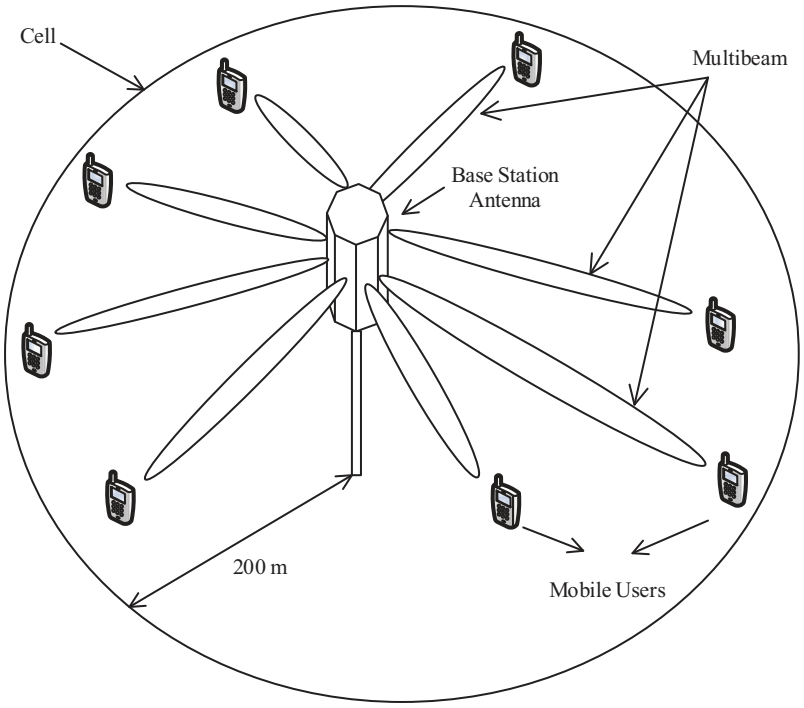

Figure 1. A multibeam base station.

Previous studies on the Butler matrix focused on the improvement of circuit performance and size reduction of the structure at frequencies below 10 GHz by eliminating some circuit elements [20–23]. Babale et al. [20] developed a 4×4 Butler matrix using modified quadrature hybrids at 6 GHz. In [21], a 4×4 Butler matrix using conductor-backed coplanar waveguide technology was designed without crossover at 5.8 GHz. Furthermore, Tian et al. [22] designed a 4×4 Butler matrix using quadrature hybrids and crossovers at 6 GHz. Although these research works successfully reduced the number of circuit elements, these techniques were only valid for a 4×4 Butler matrix and were not applicable for higher-order Butler matrices, as the structures of these matrices are more complex and difficult to design. In addition, the wavelength of the millimeter wave is very small. Therefore, the size of the Butler matrix is sufficient for mounting at the base station.

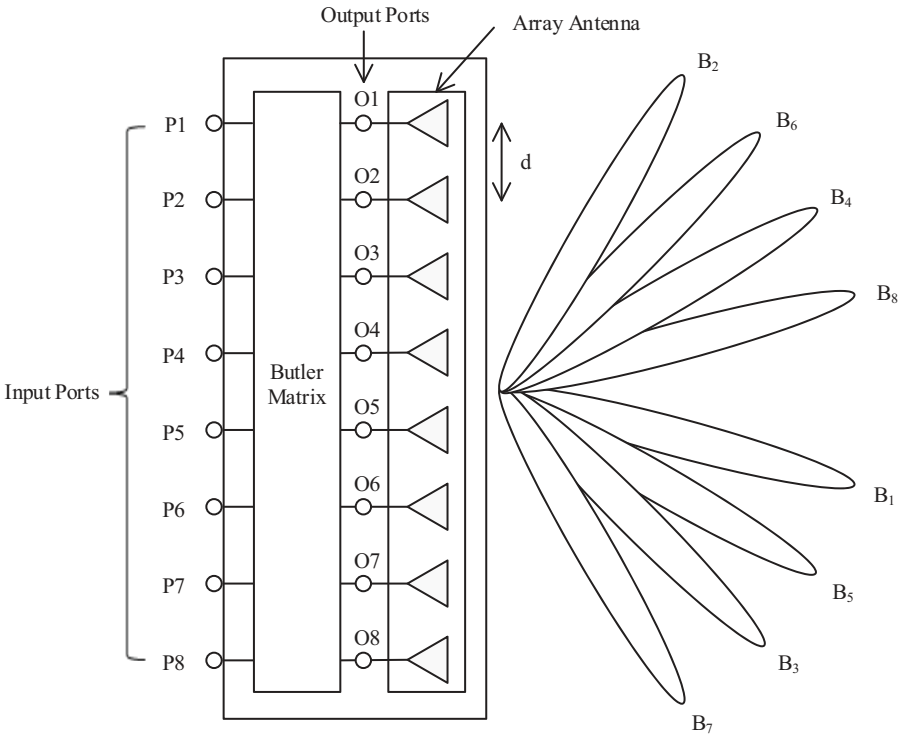

Figure 2. The configuration of a base station antenna.

Furthermore, a few studies have investigated the use of 8×8 Butler matrices based on multilayer technology. Zhai et al. [24] designed an 8×8 Butler matrix at 4.3 GHz using six quadrature hybrids and four phase shifters placed at the top and bottom layers, respectively. These layers were connected via through-holes and the results showed an insertion loss and a phase error of 2.5 dB and $\pm15^\circ$, respectively. In [25], a multibeam array antenna was fed by an 8×8 Butler matrix based on a dual layer substrate integrated waveguide from 28 GHz to 31 GHz. The proposed Butler matrix consisted of an additional four quadrature hybrids as compared to the conventional configuration. The results showed an insertion loss and a phase difference error of 2 dB and $\pm15^\circ$, respectively. The air gap between substrate layers can cause additional losses and phase errors, which could degrade the performance of the Butler matrix. Moreover, the use of through-holes in multilayer technology increases fabrication difficulties. Based on the literature, the most attractive option to overcome these issues is to use a single-layer microstrip structure, which is cost-effective and simple in design.

In this paper, the design of a single-layer multibeam array antenna fed by an 8×8 Butler matrix operating at 28 GHz is explained in detail. The multibeam array antenna was designed using Computer Simulation Technology Microwave Studio. The performance of the designed antenna was validated via fabrication and measurement. Both the simulation results and measurement results are presented and discussed in the last section of this paper.

2. Design of the Butler matrix

The Butler matrix is a passive feeding network of N inputs (Pi) and N outputs (Oi) connected to antenna elements, where N is the power of 2 ($N = 2^n$) [9]. Figure 3 shows the structure of an 8×8 Butler matrix with

eight antenna elements. The 8×8 Butler matrix consists of twelve quadrature hybrids, sixteen crossovers, and eight phase shifters. The Butler matrix has equal amplitudes at the output ports when the input port is fed. The phase differences between output ports are given by Equation (1) [26]:

$$\phi_p = \pm\frac{2p-1}{N}\times 180^\circ, \tag{1}$$

where $N=8$, $n=3$, and $p=1,2,,(n+1)$. The Butler matrix produced eight beams at eight different angles. The beam angles can be expressed using Equation (2) [27]:

$$\sin\theta_p = \pm\frac{\lambda}{d}\frac{\phi_p}{360^\circ}, \tag{2}$$

where λ is the wavelength, ϕ_p is the phase difference, and d is the antenna spacing. Table 1 lists the phase differences between the antenna elements and the beam angles for each input port.

Table 1. Phase differences between antenna elements and beam angles for each beam number.

Beam number	ϕ_p	θ_p
1	-22.5°	6°
2	157.5°	-47°
3	-112.5°	31°
4	67.5°	-18°
5	-67.5°	18°
6	112.5°	-31°
7	-157.5°	47°
8	22.5°	-6°

The structure of the 8×8 Butler matrix presented in Figure 3 was designed using Computer Simulation Technology Microwave Studio. The substrate used in this work was NPC-F220A from Nippon Pillar Packing Co. Ltd. with a substrate thickness of 0.254 mm, a dielectric constant of 2.2, and a loss tangent of 0.0007. Figure 4 shows the complete design structure of the 8×8 Butler matrix. This structure has eight input ports (P1 to P8) and eight output ports (O1 to O8).

Figure 5 presents the simulated return losses for the input and output ports of the 8×8 Butler matrix for 27 GHz to 29 GHz. The return losses were less than -10 dB for the entire frequency range. The simulated isolations between the input ports of the 8×8 Butler matrix are illustrated in Figure 6 and the isolations were less than -15 dB at 28 GHz. Figures 7–7d demonstrate the simulated insertion losses when the Butler matrix is fed at ports P1, P2, P3, and P4, respectively. Based on these figures, the average output amplitude was -11.5 dB at 28 GHz. When a signal is fed to the input port, the output amplitude at each output port is -9 dB. Therefore, the average insertion loss was 2.5 dB. The insertion loss is due to the conductor loss in the Butler matrix. However, the value of insertion loss is an acceptable level considering the operating frequency and the number of circuit elements in the 8×8 Butler matrix. Owing to the symmetrical structure of the Butler matrix, the performances of ports P5, P6, P7, and P8 were similar, so these were not presented in this paper. Figure 8 shows the simulated phase differences for the input ports from 27 GHz to 29 GHz with an average phase error of less than $\pm10^\circ$. The phase difference is the difference between the output phases of the Butler matrix. The power flow of the 8×8 Butler matrix is illustrated in Figure 9. The power from port P1 was distributed to the output ports.

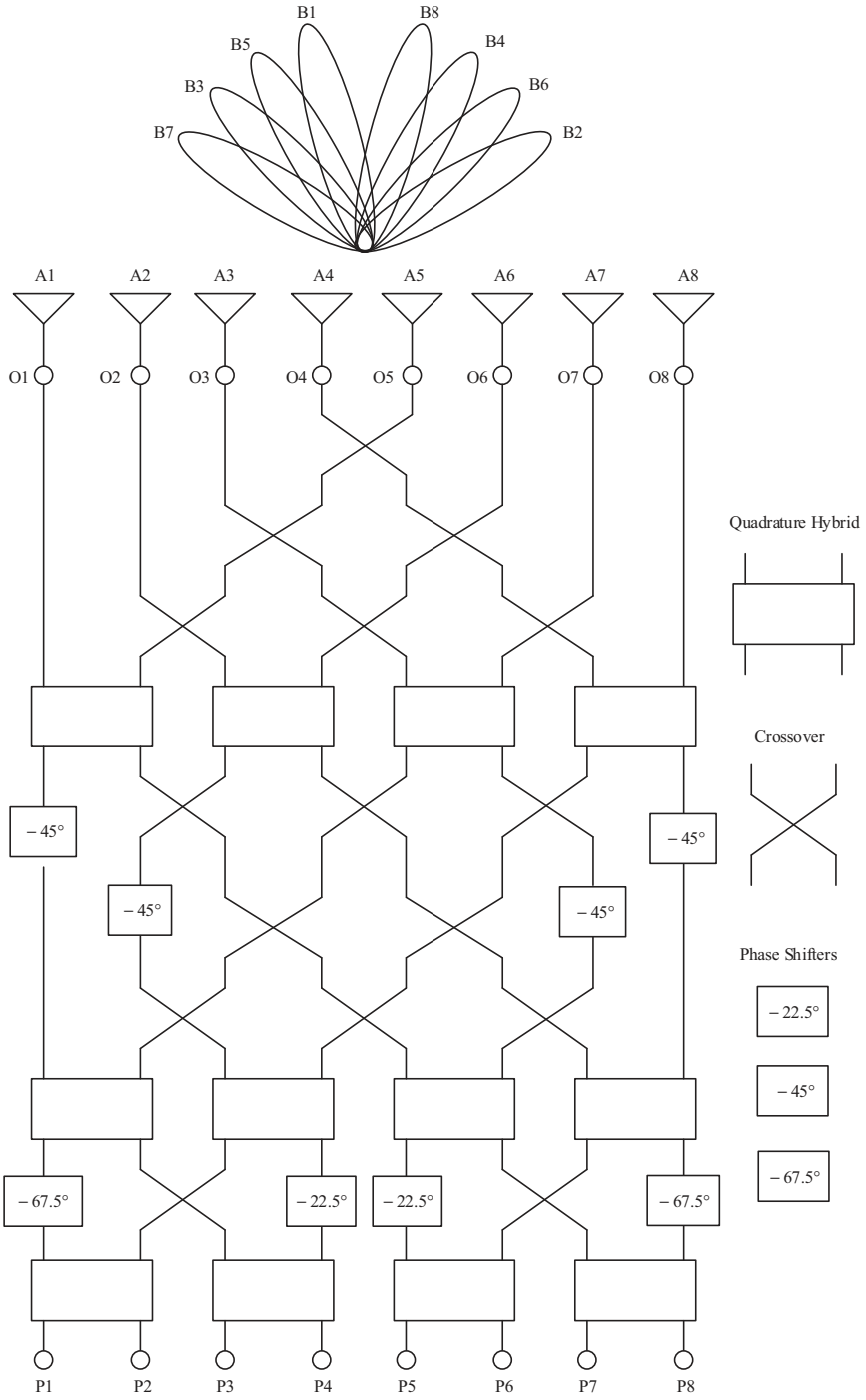

Figure 3. The structure of an 8×8 Butler matrix with eight antenna elements.

3. Design of antenna element

The microstrip antenna was designed using Computer Simulation Technology Microwave Studio. The geometry of a microstrip antenna is shown in Figure 10. The antenna was fed at the center of the antenna edge by a

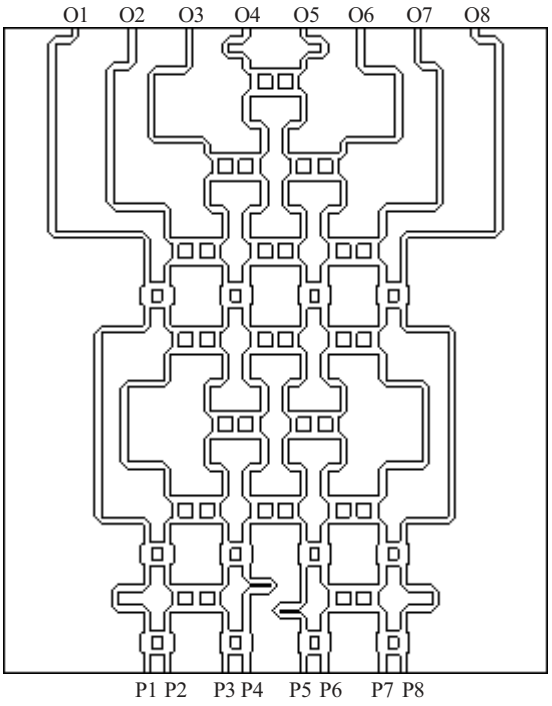

Figure 4. Designed structure of the 8×8 Butler matrix.

50 Ω microstrip transmission line with a quarter wave transformer. The quarter wave transformer was used to provide good impedance matching between the microstrip transmission line and the antenna. The optimized parameters and the characteristics of the microstrip antenna are listed in Table 2.

Table 2. Optimized parameters and characteristics of the microstrip antenna.

Structure	Parameter	Value (mm)	Characteristic
Patch	L_p	3.2529	Gain, $G_p = 7$ dBi
	W_p	4.2352	
Quarter wave transformer	L_q	2.0251	Impedance, $Z_q = 106$ Ω
	W_q	0.1984	
Microstrip feed line	L_f	1.9581	Impedance, $Z_f = 50$ Ω
	W_f	0.7826	

Figure 11 presents the simulated return loss of the microstrip antenna. The return loss was less than −10 dB from 27.6 GHz to 28.3 GHz. The radiation patterns of the microstrip antenna at 28 GHz for Phi=0° and Phi=90° are illustrated in Figures 12a and 12b, respectively. The radiation pattern of the microstrip antenna showed good symmetry at the bore sight with a gain of 7 dBi.

4. Design of multibeam array antenna

The structure of a multibeam array antenna fed by the 8×8 Butler matrix is illustrated in Figure 13a. The antenna spacing of the proposed multibeam array antenna was 0.6λ to reduce the mutual coupling between

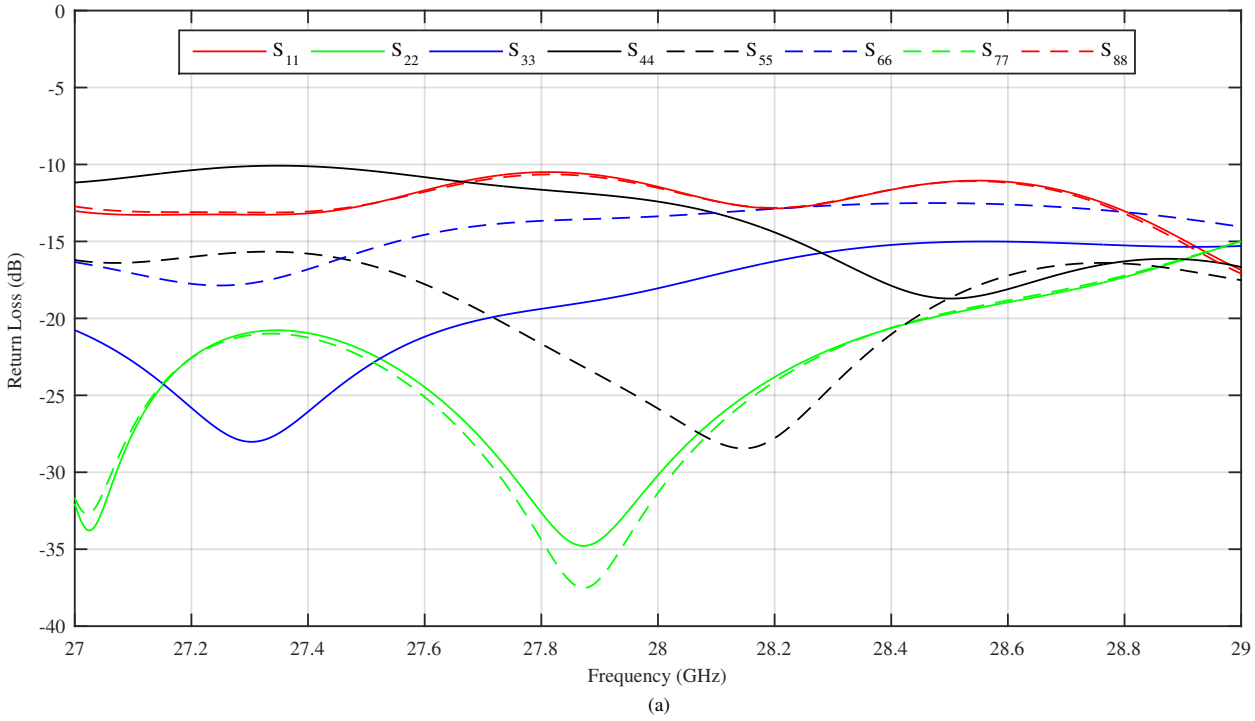

(a)

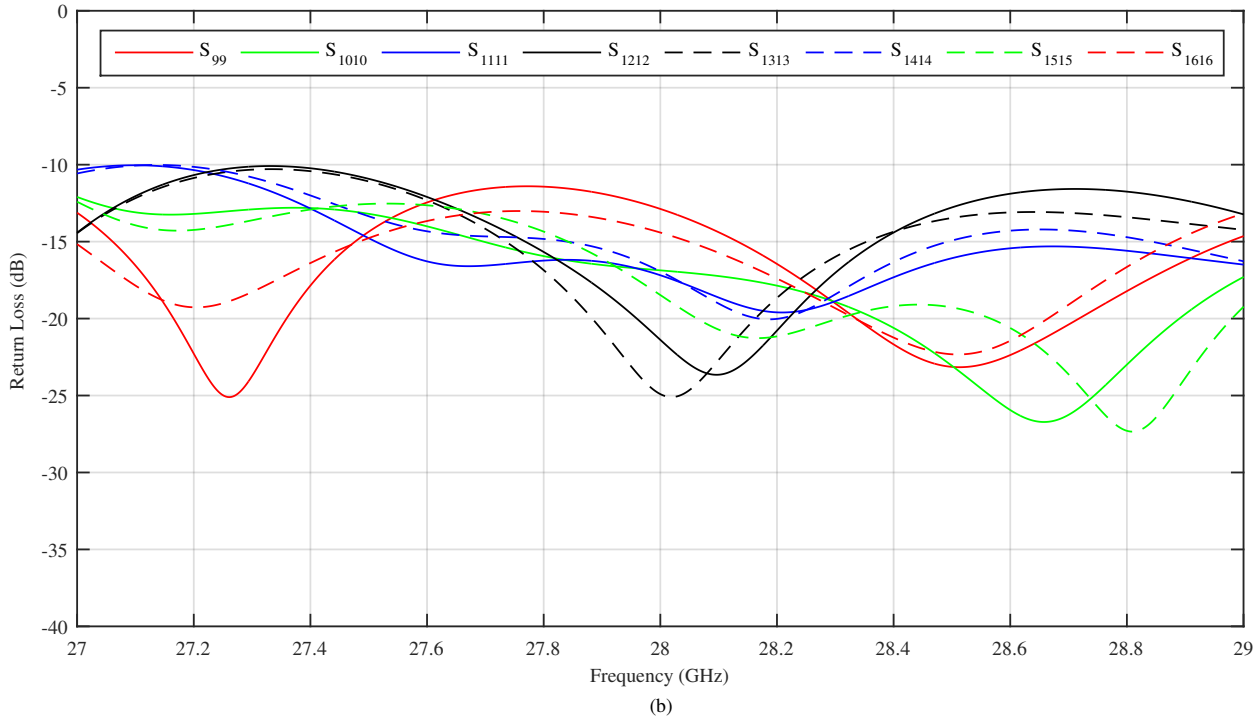

(b)

Figure 5. Simulated return losses for the (a) input and (b) output ports of the 8×8 Butler matrix.

antenna elements. In this design, the extended lines were designed at the input ports of the multibeam array antenna to allow the implementation of coaxial connectors. Figure 13b shows a photograph of the fabricated

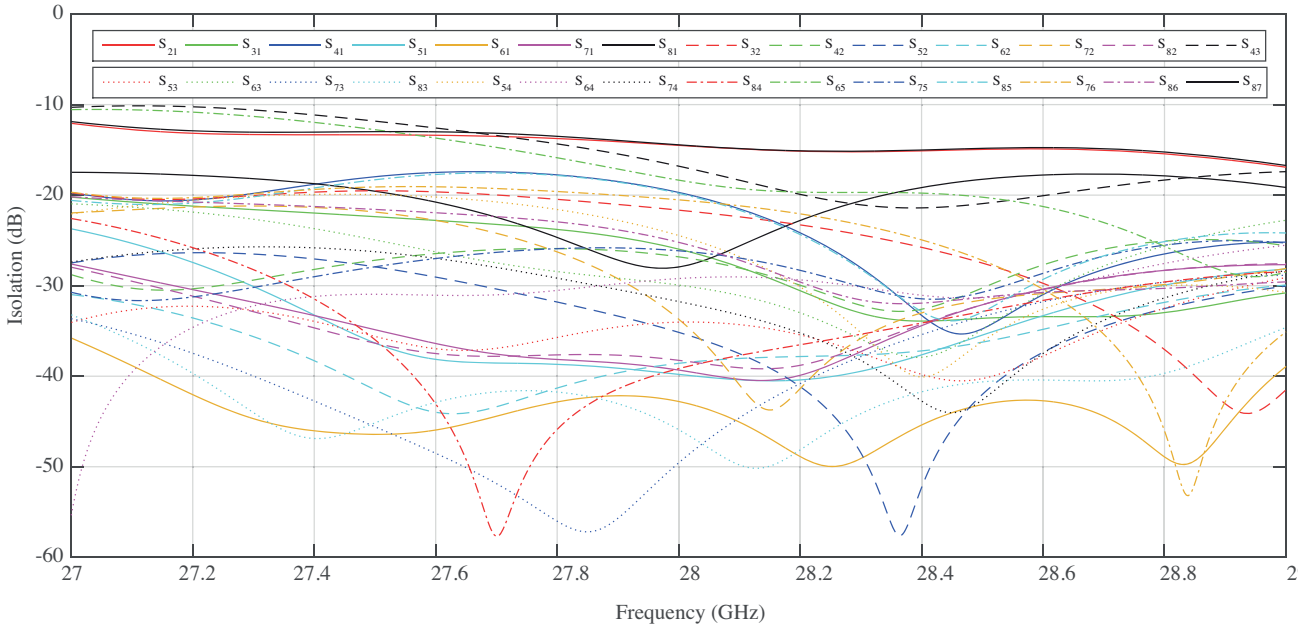

Figure 6. Simulated isolations between the input ports of the 8 × 8 Butler matrix.

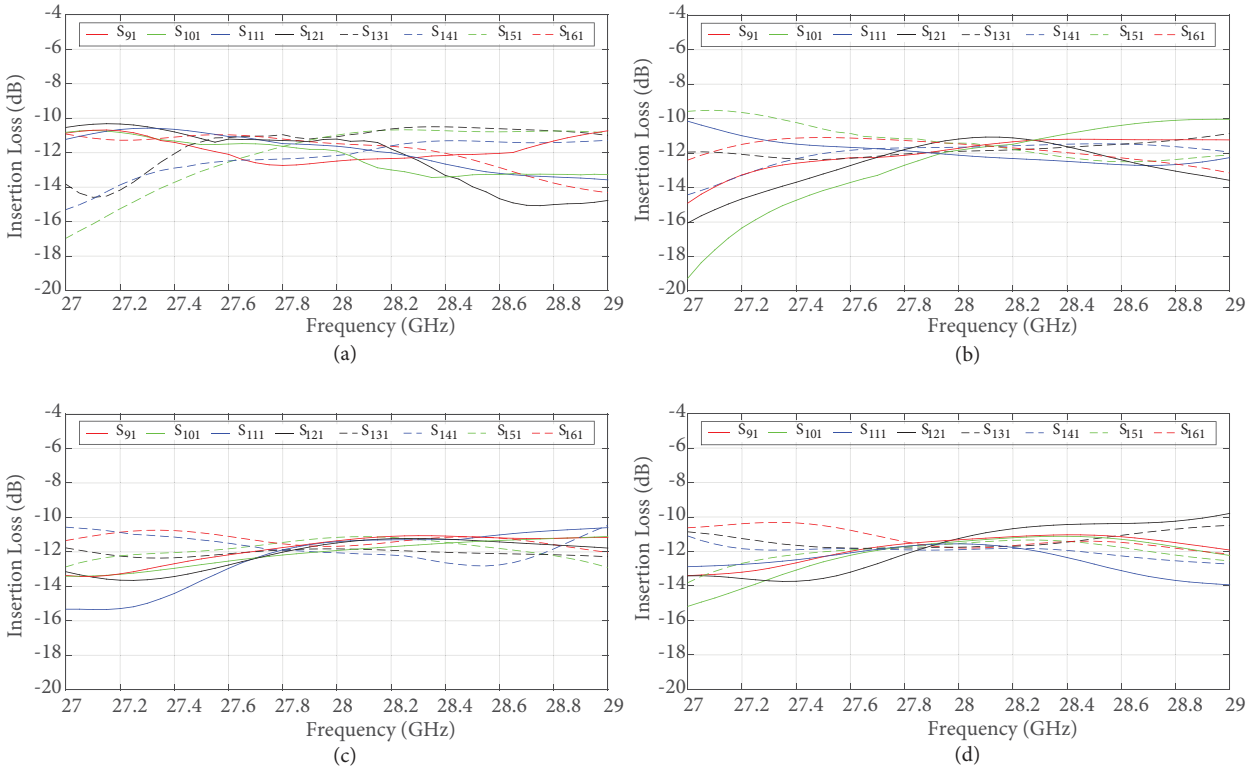

Figure 7. Simulated insertion losses of the 8 × 8 Butler matrix for ports (a) P1, (b) P2, (c) P3, and (d) P4.

multibeam array antenna. The 2.92 mm coaxial connectors were used at the input ports of the multibeam array antenna. The dimensions of the fabricated multibeam array antenna were 88 mm (width) × 106 mm (length).

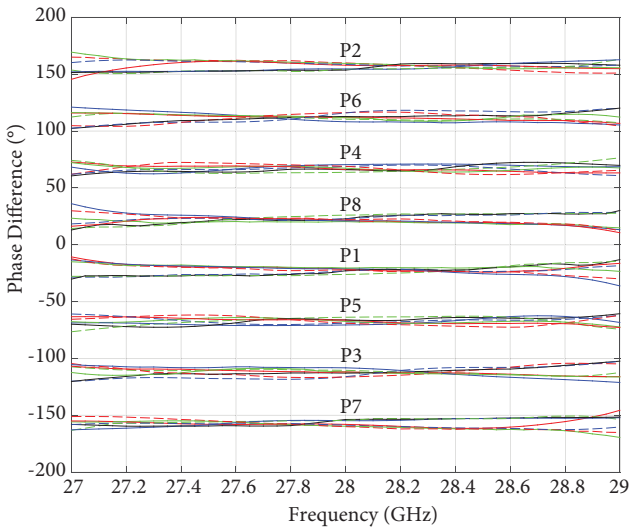

Figure 8. Simulated phase differences for the input ports of the 8 × 8 Butler matrix.

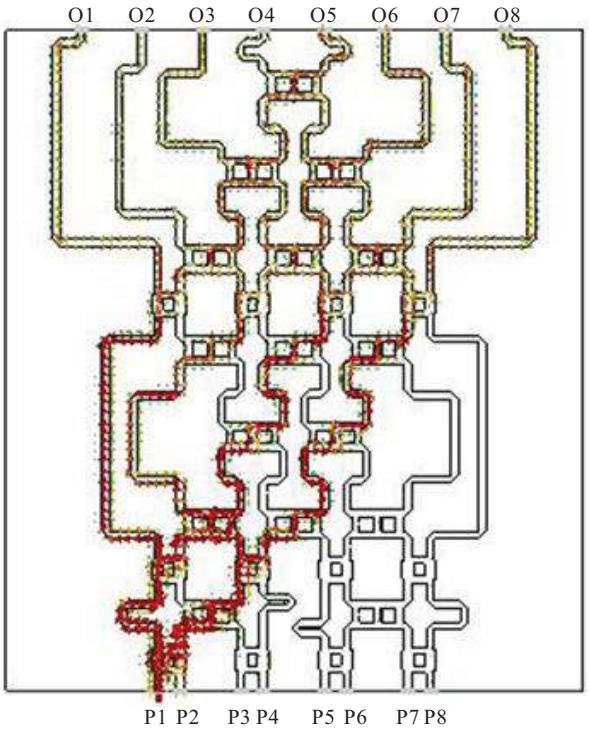

Figure 9. Power flow of the 8 × 8 Butler matrix.

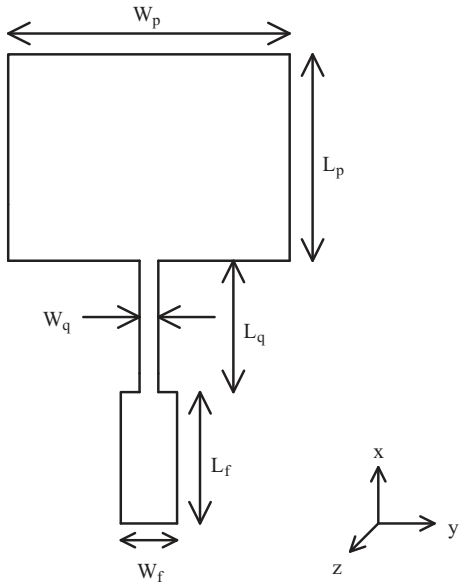

Figure 10. Geometry of a microstrip antenna.

5. Results and discussion

To validate the simulation results, the reflection coefficients of the fabricated multibeam array antenna were measured using a vector network analyzer (Keysight N5224A) and the radiation characteristics were studied in an anechoic chamber.

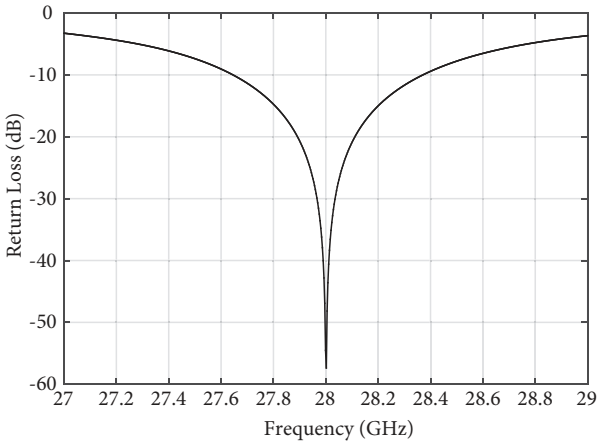

Figure 11. Simulated return loss of the microstrip antenna.

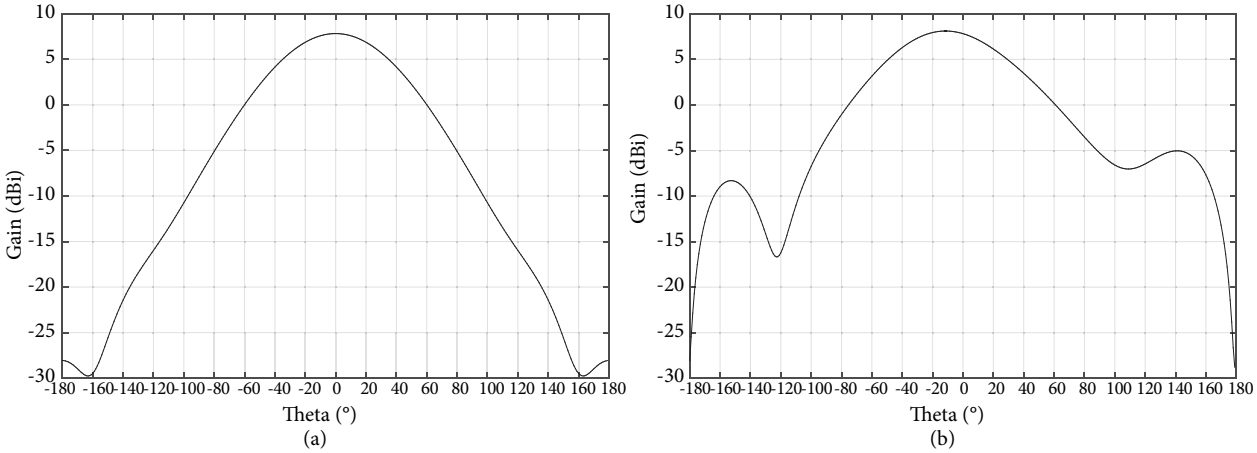

Figure 12. Simulated radiation patterns of the microstrip antenna at 28 GHz for (a) Phi=0° and (b) Phi=90°.

5.1. Reflection coefficient

Figures 14a and 14b show the simulated and measured return losses of the multibeam array antenna for each input port, respectively. The simulated and measured return losses were less than −10 dB between 27 GHz and 29 GHz. However, it can be observed that the measured results were slightly different from the simulated results due to the loss caused by the coaxial connectors.

5.2. Radiation characteristics

To ensure that the beams were pointed in the desired directions, the simulated and measured output phases for each input port of the Butler matrix are presented in Figures 15a and 15b, respectively. Both simulated and measured output phases for the input ports showed linear characteristics. Figures 16a and 16b illustrate the simulated and measured radiation patterns of the multibeam array antenna for the input ports at 28 GHz, respectively. The simulated main beams were pointed at ±5°, ±19°, ±29°, and ±46°. Meanwhile, the measured main beams were pointed at ±6°, ±18°, ±30°, and ±44°. The simulated and measured main beam angles of the multibeam array antenna agreed very well with the theoretical values, as shown in Table 1.

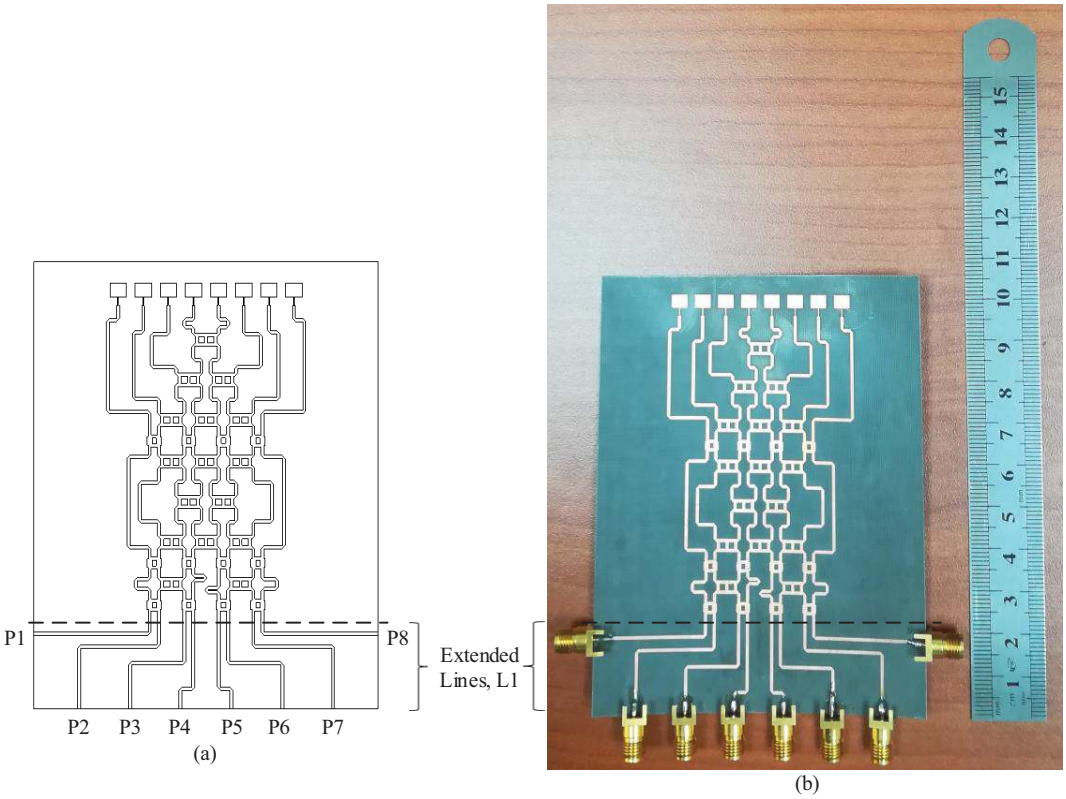

Figure 13. (a) Structure of the multibeam array antenna and (b) photograph of the fabricated multibeam array antenna.

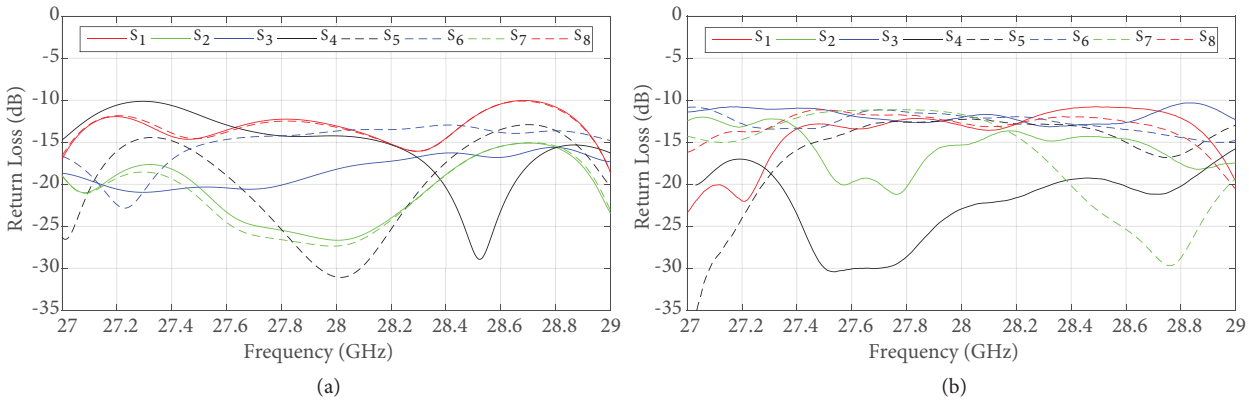

Figure 14. (a) Simulated and (b) measured return losses for the input ports of the multibeam array antenna.

The simulated and measured beam coverages of the multibeam array antenna were 92° and 88°, respectively. In addition, it can be observed that the measured side lobe characteristics were in good agreement with the simulated results. The simulated and measured gains for the input ports of the multibeam array antenna at 28 GHz are listed in Table 3. The gains were in the range of 9 dBi to 15 dBi. The differences between the simulated gains and the measured gains were less than 2 dBi.

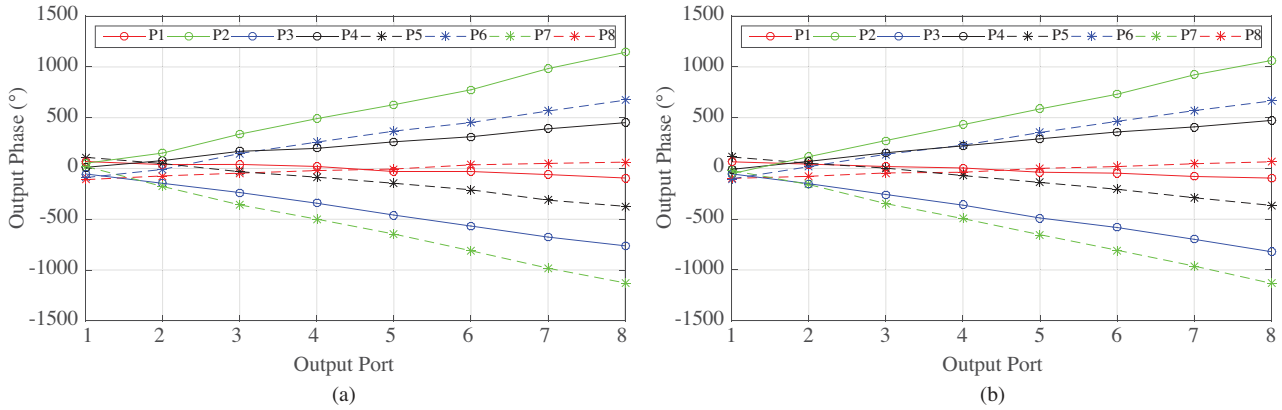

Figure 15. (a) Simulated and (b) measured output phases for the input ports of the 8×8 Butler matrix at 28 GHz.

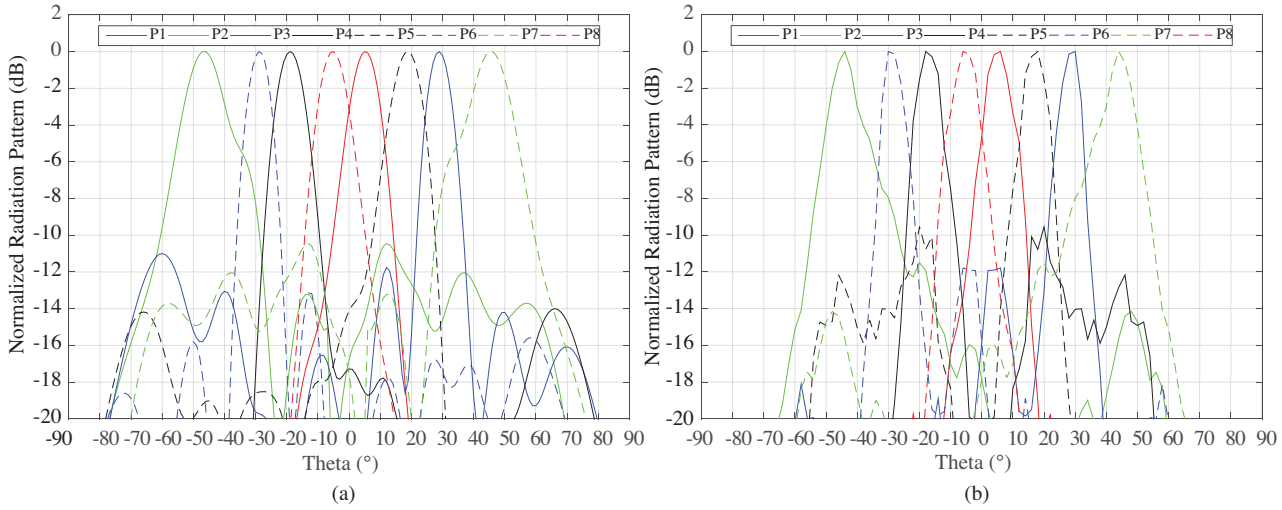

Figure 16. (a) Simulated and (b) measured main beam radiation patterns at 28 GHz for the input ports of the multibeam array antenna.

Table 3. Simulated (G_s) and measured (G_m) gains for the input ports of the multibeam array antenna.

Port number	P_1	P_2	P_3	P_4	P_5	P_6	P_7	P_8
G_s (dBi)	15.2	9.2	11.7	14.5	14.5	11.7	9.2	15.2
G_m (dBi)	14.2	9.0	10.3	12.9	12.9	10.3	9.0	14.2

6. Conclusion

In this paper, the design of a multibeam array antenna fed by an 8×8 Butler matrix based on a single-layer structure operating at 28 GHz was proposed. The structure of the multibeam array antenna was designed to be compact with dimensions of $88 \times 106 \times 0.254$ mm^3, suitable for a practical space-constrained base station. The multibeam array antenna was designed and the electric performances were ensured via comprehensive simulations. The proposed multibeam array antenna was fabricated using a low dielectric constant and a low loss tangent substrate material called NPC-F220A. The return losses were less than −10 dB at 28 GHz. The average insertion loss and phase error were 2.5 dB and ±10° at 28 GHz, respectively. The radiation

characteristics of the main beam angle for each input port showed good agreement with the simulation results. The measured gains were in the range of 9 dB to 14 dB with beam coverage of 88°. Thus, the proposed multibeam array antenna in this work is adequate and suitable for 5G mobile base station applications.

Acknowledgment

This work was supported by the University of Malaya (BK043-2017).

References

[1] Alnoman A, Anpalagan A. Towards the fulfillment of 5G network requirements: technologies and challenges. Telecommunication Systems 2017; 65: 101-116.

[2] Gavrilovska L, Rakovic V, Atanasovski V. Visions towards 5G: technical requirements and potential enablers. Wireless Personal Communications 2016; 87: 731-757.

[3] Rappaport TS, Sun S, Mayzus R, Zhao H, Azar Y et al. Millimeter wave mobile communications for 5G cellular: It will work! IEEE Access 2013; 1: 335-349.

[4] Wang C, Haider F, Gao X, You X, Yang Y et al. Cellular architecture and key technologies for 5G wireless communication networks. IEEE Communications Magazine 2014; 52: 122-130.

[5] Hong W, Jiang ZH, Yu C, Zhou J, Chen P et al. Multibeam antenna technologies for 5G wireless communications. IEEE Transactions on Antennas and Propagation 2017; 65 (12): 6231-6249.

[6] Kim JS, Shin JS, Oh S, Park A, Chung MY. System coverage and capacity analysis on millimeter-wave band for 5G mobile communication systems with massive antenna structure. International Journal of Antennas and Propagation 2014; 2014: 1-11.

[7] Wu Z, Wu B, Su Z, Zhang X. Development challenges for 5G base station antennas. In: 2018 International Workshop on Antenna Technology; Nanjing, China; 2018. pp. 1-3.

[8] Yang P, Liu D, Zhang Y. Performance analysis of joint base-station multiantenna multibeam and channel assignment scheme for hierarchical cellular system. International Journal of Antennas and Propagation 2014; 2014: 1-9.

[9] Butler JL. Multiple Beam Antennas. Nashua, NH, USA: Sanders Associates, 1960.

[10] Rotman W, Turner R. Wide-angle microwave lens for line source applications. IEEE Transactions on Antennas and Propagation 1963; 11 (6): 623-632.

[11] Blass J. Multidirectional antenna - A new approach to stacked beams. In: 1958 IRE International Convention Record; New York, NY, USA; 1960. pp. 48-50.

[12] Bantavis PI, Kolitsidas CI, Empliouk T, Roy ML, Jonsson BLG et al. A cost-effective wideband switched beam antenna system for a small cell base station. IEEE Transactions on Antennas and Propagation 2018; 66 (12): 6851-6861.

[13] Slomian I, Wincza K, Staszek K, Gruszczynski S. Folded single-layer 8×8 Butler matrix. Journal of Electromagnetic Waves and Applications 2017; 31 (14): 1386-1398.

[14] Ali AAM, Fonseca NJG, Coccetti F, Aubert H. Design and implementation of two-layer compact wideband Butler matrices in SIW technology for Ku-band applications. IEEE Transactions on Antennas and Propagation 2011; 59 (2): 503-512.

[15] Nedil M, Denidni TA, Talbi L. Novel Butler matrix using CPW multilayer technology. IEEE Transactions on Microwave Theory and Techniques 2006; 54 (1): 499-507.

[16] Zhu H, Sun H, Ding C, Guo YJ. Butler matrix based multi-beam base station antenna array. In: 2019 13th European Conference on Antenna and Propagation; Krakow, Poland; 2019. pp. 1-4.

[17] Katagi T, Mano S, Sato S. An improved design method of Rotman lens antennas. IEEE Transactions on Antennas and Propagation 1984; 32 (5): 524-527.

[18] Lee JJ, Valentine GW. Multibeam array using Rotman lens and RF heterodyne. In: IEEE Antennas and Propagation Society International Symposium; Baltimore, MD, USA; 1996. pp. 1612-1615.

[19] Bhowmik W, Srivastava S, Prasad L. Design of multiple beam forming antenna system using substrate integrated folded waveguide (SIFW) technology. Progress in Electromagnetics Research B 2014; 60: 15-34.

[20] Babale SA, Rahim SKA, Barro OA, Himdi M, Khalily M. Single layered 4×4 Butler matrix without phase-shifters and crossovers. IEEE Access 2018; 6: 77289-77298.

[21] Ben Kilani M, Nedil M, Kandil N, Denidni T. Novel wideband multilayer Butler matrix using CB-CPW technology. Progress In Electromagnetics Research C 2012; 31: 1-16.

[22] Tian G, Yang J, Wu W. A novel compact Butler matrix without phase shifter. IEEE Microwave and Wireless Components Letters 2014; 24 (5): 306-308.

[23] Traii M, Nedil M, Gharsallah A, Denidni TA. A new design of compact 4×4 Butler matrix for ISM applications. International Journal of Microwave Science and Technology 2008; 2008: 1-7.

[24] Zhai Y, Fang X, Ding K, He F. Miniaturization design for 8×8 Butler matrix based on back-to-back bilayer microstrip. International Journal of Antennas and Propagation 2014; 2014: 1-7.

[25] Zhong L, Ban Y, Lian J, Yang Q, Guo J et al. Miniaturized SIW multibeam antenna array fed by dual-layer 8×8 Butler matrix. IEEE Antennas and Wireless Propagation Letters 2017; 16: 3018-3021.

[26] Moody H. The systematic design of the Butler matrix. IEEE Transactions on Antennas and Propagation 1964; 12 (6): 786-788.

[27] Néron J, Delisle G. Microstrip EHF Butler matrix design and realization. ETRI Journal 2005; 27: 788-797.